Coexistence of FDD Flexible Duplexing Networks

S. Lembo, O. Tirkkonen
School of Electrical Engineering
Aalto University, Finland
{sergio.lembo / olav.tirkkonen}@aalto.fi

M. Goldhamer
4GCelleX, Israel
mariana@4GCelleX.com

A. Kliks
Chair of Wireless Communications
Poznan University of Technology, Poland
adrian.kliks@put.poznan.pl

***Abstract*—We study the coexistence of FDD flexible duplexing systems, where a cellular network may use FDD uplink band for downlink transmission. As a result, adjacent channel emissions will change, with an effect to networks operating on adjacent channels. To stabilize the adjacent channel interference, equalizing downlink power control is considered, such that a flexible duplexing cell radiates in downlink a power density which is equivalent to the mean uplink transmit power of the cell. We derive a closed form equation for the transmit power, and evaluate coexistence performance in a heterogeneous network using the proposed power control.**

I. Introduction

Allocation of uplink (UL) and downlink (DL) spectrum for frequency-division duplexing (FDD) transmission in mobile services, is based on the assumption of a symmetric voice traffic. Equal frequency partitions are assigned specifically for UL and DL transmission by spectrum regulators. Due to the current and future demand for asymmetric traffic [1], mainly for downlink, a new study item was proposed in 3GPP to study the feasibility of using FDD-UL spectrum for downlink transmission [2][3][4]. The proposed technology is referred to as *FDD flexible duplexing*. Flexible duplexing in frequency is an evolutionary step in the LTE road-map for flexibility in duplexing and dynamic spectrum sharing [5]. FDD flexible duplexing presents challenges of regulatory approval, User Equipment (UE) receiver functionality in uplink band, and co-existence due to Co-Channel Interference (CCI) and Adjacent Channel Interference (ACI).

From regulatory perspective, the challenge is the approval of downlink transmission in the uplink band. In some countries the regulations are stated in terms of allowed emissions for some bands [4], which could be acceptable for low power small cells, with a downlink transmission level comparable to the UE uplink transmission power [3]. A main technical challenge is coexistence in terms of CCI and ACI. CCI originates from downlink transmission in a network with neighboring cells operating in uplink. High levels of ACI appear from the fact that uplink bands in FDD uplink spectrum are assigned with a narrow frequency gap in-between, in contrast to the considerable frequency gap allocated between the portions of uplink and downlink FDD spectrum. In FDD flexible duplexing, such narrow gaps bring the problem of significant Out-of-Band (OOB) downlink emissions to the neighbor channels operating in uplink.

978–1–5386–3873–6/17/$31.00

FDD flexible duplexing was studied mainly in the context of co-channel interference. In [6], a scheme is proposed where macro cells operate in FDD, while the underlying femtocells employ Time Division Duplex (TDD) in FDD uplink or downlink band. In [7], the authors propose to make downlink transmission in the middle of an uplink frame in FDD-UL. To the best of our knowledge, coexistence between systems operating with different duplex modes in adjacent FDD bands was not properly studied.

Coexistence problems in FDD are similar to the ones encountered in adjacent-channel UL/DL crossed slots in TDD. Initial understanding can be acquired from existing research, e.g. [8]. The most notable problem in TDD is the interference between Base Stations (BS), in which a so-called aggressor BS transmits in downlink, and interferes a victim BS receiving in uplink [5]. BS-BS interference can be CCI or ACI toward BSs in a neighboring TDD frequency band. Interference analysis of the BS-BS case reveals that there is a coexistence problem if the two BSs are closer than a proximity distance recommended for a given downlink transmit power [9] [10]. There are different proposals to deal with the interference, of which downlink power control is of particular interest for implementing low power downlink transmission. In [11], the authors propose a downlink power control scheme, in which the goal is to maximize downlink throughput, subject to the constraint of keeping the uplink throughput loss of the neighbor band below a given threshold.

In this paper, we study coexistence of FDD flexible duplexing networks, where the uplink band is used for downlink transmission, considering the effect of adjacent channel emissions. We study downlink power control with the objective to make the cell implementing flexible duplexing behave, interference-wise, as an uplink cell. A simple solution is presented with a closed form equation, in which the flexible duplexing cell radiates in downlink the equivalent mean uplink transmit power, considering a uniform distribution of users in the cell. Performance when assigning this power for downlink is evaluated by simulations in a heterogeneous network.

This paper is organized as follows: Section II presents the problem formulation for FDD flexible duplexing and describes the system model. In Section III, the mean transmit power for users in uplink is presented. Section IV presents system simulations and results. Finally, Section V summarizes the main conclusions of this study.

II. Problem Formulation and System model

We consider two network operators, operator 1 and 2, which are allowed to transmit in two neighboring FDD-UL bands, 1 and 2. First we simplify by studying the case where operator 1 has one BS, BS_1, and one user, UE_1. Analogously, operator 2 has BS_2 and UE_2 (see Fig. 1). Operator 1 always uses band 1 for uplink transmission. Operator 2 uses band 2 for uplink or downlink transmission in a *flexible duplexing cell*. The figure depicts the interference situation when the flexible duplexing cell is in a) uplink, and, b) downlink.

At a given time instant when the flexible duplexing cell is in uplink, a user is scheduled for uplink transmission in radio resources at the left-most side of band 2. Other users may be scheduled for uplink in the remaining part of band 2, but we focus now on the left-most resources because this is the most notable source of OOB ACI emissions toward band 1. We do not make a concrete assumption about the arrangement of resources, uplink transmission can be data or control information. The upper part of Fig. 1 represents the transmit power at UE_2, and the received power at BS_1. BS_1 receives in band 1, ideally, all the uplink transmissions at a target received power level P_0, which is achieved by uplink power control of its users. BS_1 receives also in band 1 the OOB emissions leaked from band 2. Due to the relative low uplink power of UE_2 and the propagation loss, the OOB emissions that invade band 1 are on an acceptable level.

If operator 2 switches it's BS_2 to downlink transmission in band 2, with a relative high power, the OOB emissions leaked to band 1 may become a significant source of interference to band 1. The lower part of Fig. 1 represents the transmit power at BS_2, and the received power at BS_1. A significant amount of ACI from band 2 invades band 1. In this setting we call BS_2 *aggressor BS*, and BS_1 *victim BS*. For convenience, we will call BS_1 victim BS also when the flexible duplexing cell is in uplink.

The permissible level of OOB emissions is regulated and stated by spectrum emission masks (SEM) and Adjacent Channel Leakage power Ratios (ACLR). In LTE, ACLR is the ratio of the filtered mean powers measured at the centers of two adjacent bands. Allowed emissions enforced by ACLR are measured from the band edges [12][13]. We adopt ACLR as a convenient measure to restrict emissions after the band edge, and for simplicity consider that OOB emissions are flat, at a level calculated from ACLR, and extending to the center of the adjacent band. As numerical values we use $ACLR_{\mathrm{UL}} = 30$ dB for uplink [12], and $ACLR_{\mathrm{DL}} = 45$ dB for downlink [13]. Characteristics of the victim's receiver are the same, for interference coming from an aggressor transmitting in uplink or downlink. Ideal, perfect, receiver filter selectivity is assumed for both cases. Coexistence analysis is performed evaluating OOB interference in the Physical Resource Block (PRB), of the victim's band closest to the edge of the band.

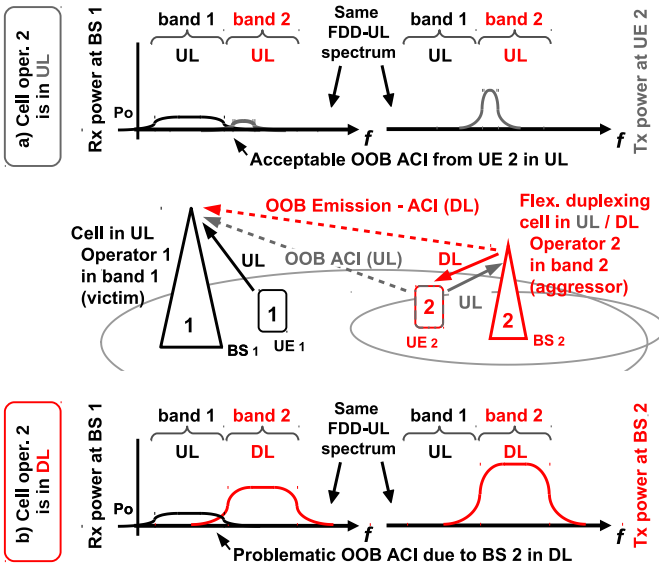

Fig. 1. Adjacent channel out-of-band emissions from operator 2's cell in a) uplink, b) downlink, received at the BS of operator 1 in uplink. User 1 and BS 1 belong to operator 1, transmitting in band 1. Analogous assignment for operator 2.

III. Downlink Power Control From Mean Uplink Power

To control ACI, we consider making the flexible duplexing cell behave, interference-wise, as in the uplink case. The simplest solution in this direction is to make the cell radiate the same mean transmit power in downlink as in uplink. Then, ideally, it is indistinguishable if the cell is operating in uplink or downlink when observed from a relative large distance. When observing the ACI of an aggressor as interference in the victim's BS, we can identify that there is a separation distance where the interference received from an aggressor's BS is larger than from an aggressor's UE. This distance is minimized when the aggressor's BS reduces the transmit power, and by adopting better filters in the BS, meaning a higher ACLR, and a relative lower ACI.

We aim to calculate the expected uplink power in a circular cell with a uniform distribution of users. For this purpose we calculate first the Probability Density Function (PDF) of the uplink transmit power.

Taking the uplink power control of LTE as reference [14], the uplink transmit power P_{dB} of a user, expressed in dBm, considering the power in one PRB, full path loss compensation and no correction parameters, is determined by

$$P_{\mathrm{dB}} = L_{\mathrm{dB}} + P_0, \tag{1}$$

where L_{dB} is the path loss from the BS to the user in dB, and P_0 is the target received power in dBm. The power in the linear domain is represented by P. We assume that there is no need to limit the power to a maximum power, which is typical for small cells and local area BSs.

The PDF of the uplink transmit power can directly be found by considering the PDF of path-losses with the linear transform (1) in the logarithmic domain. We first consider the case where a single-slope path loss model

$$L_{\mathrm{dB}} = \alpha + \beta \log_{10}(r/r_0) + \Psi \tag{2}$$

is used in an annulus. Here α is the path loss at the reference distance r_0, $\beta = 10n$, where n is the path loss exponent, r is the distance, and Ψ is a shadow fading random variable from a zero-mean Normal distribution and variance σ_Ψ^2. The PDF of the dB-domain path loss L_{dB} in an annulus with inner radius $r = R_1$, and outer radius $r = R_2$ is given by [15]

$$\begin{aligned} f_{L_{\mathrm{dB}}}(l_{\mathrm{dB}}, \mathbf{\Lambda}) =& K_1 10^{2\left(\ln(10)\sigma_\Psi^2 + \beta(l_{\mathrm{dB}} - \alpha)\right)/\beta^2} \\ & \mathrm{erfc}\left[\frac{l_{\mathrm{dB}} + K_2 - \beta \log_{10}(r)}{\sqrt{2}\sigma_\Psi}\right]\Bigg|_{R_1}^{R_2}, \end{aligned} \tag{3}$$

where l_{dB} is the path loss input to the PDF function,

$$\begin{aligned} K_1 &= \frac{r_0^2 \ln(10)}{\beta\left(R_2^2 - R_1^2\right)}, \\ K_2 &= -\alpha + \beta \log_{10}(r_0) + 2\ln(10)\sigma_\Psi^2/\beta, \end{aligned} \quad , \tag{4}$$

and $\mathrm{erfc}[\cdot]$ is the complementary error function. The parameters are collected to the vector $\mathbf{\Lambda} = [R_1; R_2; r_0; \alpha; \beta; \sigma_\Psi]$.

The PDF of the uplink transmit powers is found by changing α in the path loss equation (2) to

$$\tilde{\alpha} = \alpha + P_0, \tag{5}$$

changing variable l_{dB} to represent the transmit power p_{dB}, and collecting parameters in the vector $\tilde{\mathbf{\Lambda}} = [R_1; R_2; r_0; \tilde{\alpha}; \beta; \sigma_\Psi]$. The PDF of the uplink transmit power in dB domain is then $f_{P_{\mathrm{dB}}}\left(p_{\mathrm{dB}}, \tilde{\mathbf{\Lambda}}\right) = f_{L_{\mathrm{dB}}}\left(p_{\mathrm{dB}}, \tilde{\mathbf{\Lambda}}\right)$. Note that here we have a parameter

$$\tilde{K_2} = -\tilde{\alpha} + \beta \log_{10}(r_0) + 2\ln(10)\sigma_\Psi^2/\beta. \tag{6}$$

The expected uplink transmit power in the linear domain is

$$\mathbb{E}[P] = \int_{-\infty}^{\infty} 10^{\ p_{\mathrm{dB}}/10} f_{P_{\mathrm{dB}}}\left(p_{\mathrm{dB}}, \tilde{\mathbf{\Lambda}}\right) \mathrm{d}p_{\mathrm{dB}}, \tag{7}$$

which evaluates to

$$\mathbb{E}[P] = -K_1 e^D \left[\underbrace{\int_{-\infty}^{\infty} e^{A p_{\mathrm{dB}}} \mathrm{erf}\left[B p_{\mathrm{dB}} + C(r)\right] \mathrm{d}p_{\mathrm{dB}}}_{I(r)}\right]\Bigg|_{R_1}^{R_2}, \tag{8}$$

where

$$\begin{aligned} A &= \frac{\ln(10)\left(2\beta + \beta^2/10\right)}{\beta^2} \\ B &= \frac{1}{\sqrt{2}\sigma_\Psi} \\ C(r) &= \frac{\tilde{K_2} - \beta \log_{10}(r)}{\sqrt{2}\sigma_\Psi} \\ D &= \frac{2\ln(10)\left(\ln(10)\sigma_\Psi^2 - \tilde{\alpha}\beta\right)}{\beta^2} \end{aligned} \quad , \tag{9}$$

Integral $I(r)$ was solved in [16], with solution

$$\begin{aligned} I(r) =& \frac{1}{A}\Bigg[e^{\frac{A(A - 4BC(r))}{4B^2}} \mathrm{erf}\left(\frac{A - 2B(B\,p_{\mathrm{dB}} + C(r))}{2B}\right) \\ & + e^{A\,p_{\mathrm{dB}}} \mathrm{erf}(B\,p_{\mathrm{dB}} + C(r))\Bigg]\Bigg|_{p_{\mathrm{dB}} \to -\infty}^{p_{\mathrm{dB}} \to \infty} \end{aligned} \tag{10}$$

Taking the limits, and inserting to (10), the expected uplink power in the linear domain is,

$$\mathbb{E}[P] = \frac{2K_1 e^D}{A}\left[e^{\frac{A(A - 4BC(R_2))}{4B^2}} - e^{\frac{A(A - 4BC(R_1))}{4B^2}}\right], \tag{11}$$

where A,B, $C(\cdot)$, D are defined in (9), K_1 in (4), $\tilde{K_2}$ in (6), and $\tilde{\alpha}$ in (5).

IV. System Simulation and Results

Coexistence of two operators in FDD adjacent bands, when one operator implements FDD flexible duplexing in a small cell (SC), is studied with a custom made system simulator. We consider two networks, both with macro cells operating in uplink. One network has a small cell operating in uplink, whereas the other network has a flexible duplexing small cell, which can switch transmission from uplink to downlink. The flexible duplexing small cell is regarded as an aggressor, producing OOB emissions that interfere the network of a victim operator. We measure how this interference degrades the performance of the victim, when the aggressor operates the flexible duplexing cell for uplink and downlink transmission. Comparison of performance for the uplink and downlink cases lets us observe whether the cell implementing flexible duplexing behaves in downlink, interference-wise, as in the uplink case, and therefore can coexist. For downlink transmission power we assign the mean uplink power calculated with (11). Performance is studied by observing the Signal-to-Noise-Ratio (SINR) at a macro and small cell in the victim's network.

A. Simulation scenario

For the victim operator (operator 1) we consider a Heterogeneous Network (HetNet), based on [17], in which all the UEs communicate in uplink. The victim's network consists of seven macro cells and one small cell. We analyze the interference situation in the macro cell located at the center of the network. The six macro cells around this cell provide CCI in the victim's network. Each of these cells are separated at angular steps of 60 degrees and at a constant inter-site-distance (ISD) of 500 meters with respect to the cell at the center. Fig. 2 depicts the layout of the victim's network (dark lines). Each one of the macro cells is divided into three sectors. We concentrate on analyzing one of the sectors in the center cell, the shaded sector in the figure. Each macro cell has a macro BS in the center, which is in a fixed position. In the sector of interest there is also a small cell, which is part of the victim's HetNet, also communicating in uplink. This cell is placed in the sector following a uniform distribution, however not closer than 105 meters to the macro BS [17]. Table I summarizes the parameters for the scenario.

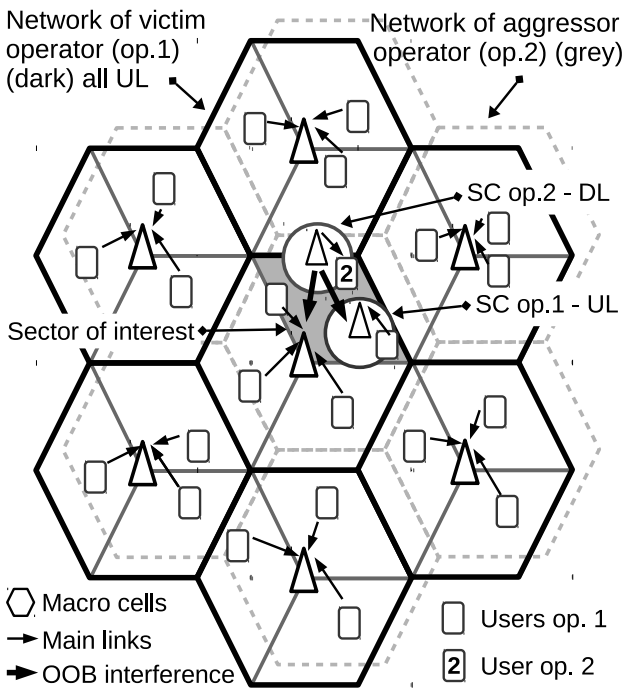

Fig. 2. HetNet layout of victim operator (op. 1), and aggressor operator (op. 2). Macro cell network of op.1 (dark) and op.2 (grey) are in uplink. Small cell of op.1 is in uplink. Flexible duplexing small cell of op.2 can be in uplink/downlink. The downlink case is represented, where thick arrows represent OOB interference to the victim's macro and small cell of interest

TABLE I
NETWORK SETTINGS

	Settings for macro {small} cells
Layout	Hexagonal grid, 3 sectors per site, 7 sites. One sector of interest in the central site used for analysis (for op. 1)
UE TX power	Determined by UL pwr. ctrl., and allocated to one PRB.
Carrier frequency	2.0GHz
Distance path loss	UMa {UMi} LOS (Table B.1.2.1-1 [18])
Shadowing	σ = 4 dB (UMa) {σ = 3 dB (UMi)}
Antenna Height:	Macro BS h_{BS} = 25 m, h_{UE} 1.5 m {SC BS h_{BS} = 5 m}
Antenna gain	17 dBi {17 dBi} for BSs / 7 dBi for UEs
Antenna configuration	SISO 1x1
Antenna pattern	Per sector, horizontal 2D, $\phi_{3\mathrm{dB}}$ = 70 deg. A_m = 25 dB [18] {Omni-directional}
Number of UEs	1 in each cell/sector {1 in SC}
UEs dropping	UEs uniformly distributed in each sector of each cell [cell]. In sector of interest one UE is assigned to macro cell and other to the SC by RSRP.
Cell radius:	500 m. {Determined by DL RSRP in op. 1, and 100 m in op. 2}
Minimum distances	Macro BS - UE: 35 m (same and diff, op.) SC - UE: 5 m (same and different op.) Macro BS - SC BS: 105 m (same op.) Macro BS - Macro BS: 35 m (different op.) Macro BS - SC BS: 15 m (different op.) SC BS - SC BS: 15 m (different op.)
Traffic model:	Full buffer
Noise figure	5 dBi {5 dBi} for BSs / 7 dBi for UEs
UE speed	None (static)
Cell selection criteria	RSRP
Target RX power	-105 dBm {-95 dBm} / 180 kHz
Thermal noise level	-174 dBm/Hz

In each sector of the macro cells a UE is dropped following a uniform distribution. In addition, a UE is dropped into the small cell. Cell association is based on downlink Reference Signal Received Power (RSRP). We measure the SINR of the UEs in the sector and small cell of interest, considering CCI and the OOB emissions of the aggressor operator in the corresponding PRB. Fig. 2 shows an example of a network instance, where UEs and links to the serving BSs are depicted. Interference links are not shown for simplicity.

The aggressor operator (operator 2) also has a HetNet. The macro cell network is analogous to the victim's network, but shifted such that the macro BS at the center of the hexagonal grid is uniformly distributed in the sector of interest, constrained to be no closer than 35 meters from the macro BS of the victim operator. Fig. 2 shows the hexagonal cells of the aggressor drawn with grey lines. An additive component of OOB emissions generated by the UEs in uplink in this network is considered. We assume that each aggressor's UE transmits in one PRB, and thus half of the PRBs available in the band contribute to an additive interference to the adjacent band. The additive effect in half of the band is consistent with the assumption that the ACI is extending flat to the middle of the adjacent band, and is observed at the edge of the victim's band. For the 10 MHz band considered here there are 50 PRBs.

In each aggressor's macro cell sector, we take a point uniformly distributed, and co-locate 25 UEs. These UEs contribute to the additive OOB interference at the victim. Co-locating the UEs, instead of distributing these independently in the sectors, was done to simplify the implementation. This assumption does not affect the study, due that the effect is a slight change in the positioning of the reference SINR distribution, which is common to the uplink and downlink cases of flexible duplexing to be studied,

The aggressor operator has a flexible duplexing small cell of radius 100 meters, which is uniformly distributed in the sector of interest, requiring that the BS is no closer than 15 meters to the victim's macro and small cell BSs. Fig. 2 depicts the small cell for the downlink case, showing only one UE, for clarity. We distribute uniformly 25 UEs in the small cell. These UEs contribute to the additive OOB emission toward the adjacent band when the small cell is in uplink. We proceed to simulate two cases, in which the small cell transmits in 1) uplink case, and 2) downlink case.

1) Flexible duplexing in uplink case: Here the small cell of the aggressor is used for uplink transmission. We assume that all the UEs associated to the aggressor's small cell causes an OOB emission with an $ACLR_{\mathrm{UL}}$ of 30 dB from the UE transmit power [13], considering uplink power control. The additive effect of the emissions is considered as interference in the calculation of the SINR at the macro and small cell of the victim operator.

2) Flexible duplexing in downlink case: Here the small cell of the aggressor is used for downlink transmission. In this case we assume that the small cell BS transmits with a downlink power per PRB, calculated from the mean uplink power of the users in the cell with (11). The level of OOB emission is calculated from the total power, i.e. the mean uplink power multiplied by the total number of 50 PRBs in the band, and attenuated with an $ACLR_{\mathrm{DL}}$ of 45 dB [12]. This emission is then considered as interference in the calculation of the SINR at the macro and small cell of the victim operator.

B. Simulation methodology

We perform a Monte Carlo simulation generating 2000 network instances. In each network instance we place UEs and small cells as stated, and then calculate the proper transmission power using uplink power control for uplink transmission. It is noted that UEs' scheduling in the time domain is abstracted by generating random network instances, and specific resource allocation is not needed, as the performance is measured in SINR. Next, path losses are calculated for each link according to the distance and antenna heights, using the propagation models listed in Table I. Finally, SINRs are calculated in each instance considering CCI and ACI, with ACI both in the case in which the aggressor's small cell is in uplink, and in downlink with different transmit powers.

C. Calculation of mean uplink transmit power

To confirm with [18] we use a two slope path loss model with a break point distance r_{BP}. To estimate the expected uplink transmit power using (11), we thus have to split the area of the cell in two rings. From the UMi model of [18], with antenna heights $h_{\mathrm{BS}} = 25$ and $h_{\mathrm{UE}} = 5$ m, we find $r_{BP} = 53$ m. Consistent with (2), for $3\ \mathrm{m} < r < r_{\mathrm{BP}}$, we calculate $\alpha^{(1)}$ and $\beta^{(1)}$, and for $r_{\mathrm{BP}} < r < 5000$ m, calculate $\alpha^{(2)}$ and $\beta^{(2)}$. The superscripts distinguish the two path loss models and the corresponding two rings. Rings have limits $R_1^{(1)} = 5$ m, $R_2^{(1)} = R_1^{(2)} = r_{\mathrm{BP}}$, and $R_2^{(2)} = 100$ m. With the two sets of parameters we calculate the mean uplink powers $\mathbb{E}[P]^{(1)}$ and $\mathbb{E}[P]^{(2)}$ via (11). The expected uplink power in the whole cell is obtained from $\mathbb{E}[P] = p_1\mathbb{E}[P]^{(1)} + p_2\mathbb{E}[P]^{(2)}$, where p_1 and p_2 are the probabilities for selecting rings 1 and 2 respectively, determined by the ring areas. The resulting expected uplink power is $\mathbb{E}[P] = -27.7$ dBm, assuming $P_0 = -95$ dBm in 180 kHz ($\mathbb{E}[P] = -10.5$ dBm / 10 MHz), to be set as downlink power in the BS.

D. Simulation results

Simulation results are presented in terms of the cumulative distribution function (CDF) of the SINRs obtained in all the network instances. Figures 3 and 4 show the CDF of the SINR measured in a PRB of the victim's macro and small cell, respectively, in the sector of interest. The observations are the same for both figures. First, we observe a baseline reference in which there is only CCI in the victim's network (curve CCI only). Second, we observe the effect of including the OOB interference of the aggressor's macro cells in uplink, as well as the OOB interference of the aggressor's small cell in uplink (curve FDD ACI). This case is the reference, against which we next compare the relative effect of implementing flexible duplexing. Third, we switch the aggressor's small cell from uplink to downlink transmission, setting the small cell BS with the downlink transmit power calculated in the previous subsection. In this case we considered downlink power control, we observe that the effect in performance is not worse than for the uplink case (dashed line labeled SCFD/PC, almost overlapping the baseline case), meaning that there is not a coexistence problem. Finally, we observe the effect of using a maximum downlink transmit power of 30 dBm in the band, as evaluated in [10]. In this case we observe that there is a coexistence problem.

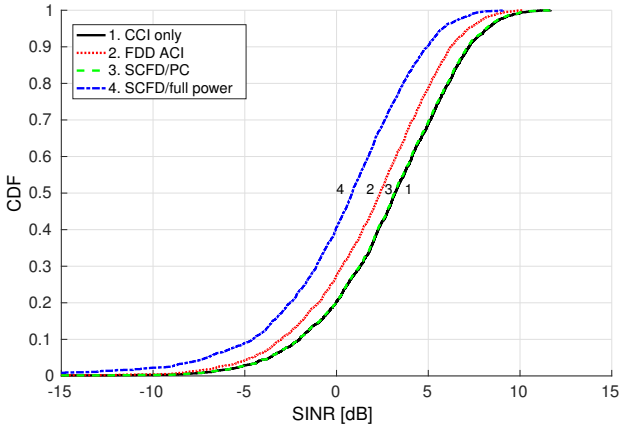

Fig. 3. SINR measured at the macro cell of the victim (op. 1), in uplink. Sources of interference: 1) CCI only, 2) CCI + FDD ACI from op. 2 macro and small cell in uplink, 3) CCI + FDD ACI from op. 2 macro cell in uplink, and small cell in downlink (Power Control, -10.5 dBm / 10 MHz), 4) Same as 3. with full power (30 dBm / 10MHz).

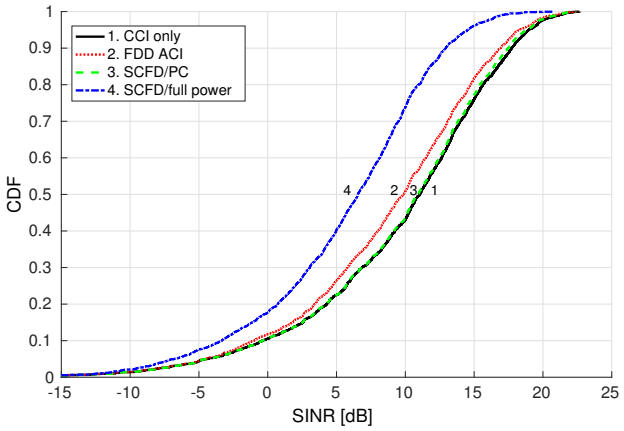

Fig. 4. SINR measured at the small cell of the victim (op. 1), in uplink. Sources of interference: 1) CCI only, 2) CCI + FDD ACI from op. 2 macro and small cell in uplink, 3) CCI + FDD ACI from op. 2 macro cell in uplink, and small cell in downlink (Power Control, -10.5 dBm / 10 MHz), 4) Same as 3. with full power (30 dBm / 10MHz).

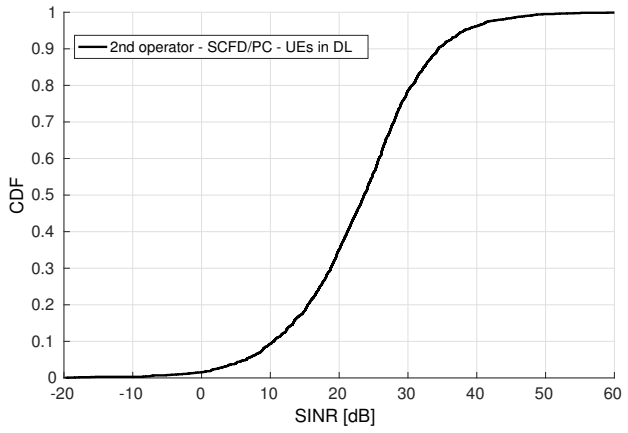

Fig. 5. SINR measured at the small cell of the aggressor (op. 2), in downlink, with transmit power -10.5 dBm / 10 MHz.

An additional evaluation is done to observe the performance of the aggressor's small cell in downlink with the transmit power calculated with (11), Fig. 5. The figure shows the performance of users in the flexible duplexing small cell, when the main source of interference are co-channel macro UEs transmitting in uplink in the aggressor's own network. The SINRs observed in the aggressor's small cells are good, making downlink operation feasible.

V. Conclusion

We studied the coexistence of FDD flexible duplexing, where the uplink band can be used for downlink transmission, considering the effect of adjacent channel emissions. We applied downlink power control such that the cell implementing flexible duplexing behaves, interference-wise, as in the uplink case, radiating in downlink the equivalent mean uplink transmit power. Then, we derived a closed form equation to calculate the mean uplink power, and finally, evaluated the effect of implementing this power in a HetNet scenario. Simulation results show that, in the considered scenario, adopting this power control produces a performance in the victim's network that is not worse than the one for uplink transmission, and therefore there is no coexistence problem. In addition, the downlink performance in the flexible duplexing small cell is good. From this, we conclude that applying flexible duplexing is a feasible method of expanding bandwidth for downlink use in small cells.

In this work we considered OOB emissions from the perspective of allowable emissions, defined by ACLR. Future work may consider a more precise modeling of OOB emissions and their additive effect. However, it is noted that resolution of SEM and ACLR levels are relatively coarse, resulting in filters of different characteristics to comply with the allowed emissions, and making a more precise study tied to specific parameters. In addition, future work will consider a trade-off between the allowed distance between the BSs of the two operators and downlink transmit power.

Acknowledgment

This work has been carried out in the framework of the H2020 project ICT-671639 COHERENT, which is funded by the European Union.

References

[1] ITU, "IMT traffic estimates for the years 2020 to 2030," Tech. Rep. Report ITU-R M.2370-0, 2015.

[2] LG Electronics and IAESI, "Discussion on dynamic traffic adaptation for LTE FDD system," Tech. Rep. 3GPP TSG-RAN 63 RP-140414, 2014.

[3] Huawei, HiSilicon, China Telecom, Unicom, and CATR, "Motivation of new SI proposal: Evolving LTE with flexible duplex for traffic adaptation," Tech. Rep. 3GPP TSG-RAN 63 RP-140426, 2014.

[4] LG Electronics, "Discussion on flexible resource utilization for LTE FDD system," Tech. Rep. 3GPP TSG-RAN 64 RP-140757, 2014.

[5] L. Wan, M. Zhou, and R. Wen, "Evolving LTE with Flexible Duplex," in *2013 IEEE Globecom Workshops (GC Wkshps)*, Dec 2013, pp. 49–54.

[6] Y. S. Soh, T. Q. S. Quek, M. Kountouris, and G. Caire, "Cognitive hybrid division duplex for two-tier femtocell networks," *IEEE Transactions on Wireless Communications*, vol. 12, no. 10, pp. 4852–4865, October 2013.

[7] A. Kliks and P. Kryszkiewicz, "Simultaneous uplink and downlink transmission scheme for flexible duplexing," in *Cognitive Radio Oriented Wireless Networks: 11th International Conference, CROWNCOM 2016, Grenoble, France, May 30 - June 1, 2016, Proceedings*, D. Noguet, K. Moessner, and J. Palicot, Eds. Springer International Publishing, 2016, pp. 192–203.

[8] P. Pirinen, "Challenges and possibilities for flexible duplexing in 5G networks," in *Computer Aided Modelling and Design of Communication Links and Networks (CAMAD), 2015 IEEE 20th International Workshop on*, Sept 2015, pp. 6–10.

[9] S. M. Heikkinen, H. Haas, and G. J. R. Povey, "Investigation of adjacent channel interference in UTRA-TDD system," in *UMTS Terminals and Software Radio, IEE Colloquium on*, 1999, pp. 13/1–13/6.

[10] 3GPP, "Feasibility study on possible additional configuration for LTE Time Division Duplex (TDD) (Release 13)," Tech. Rep. TR 36.825 V13.0.0, 2015.

[11] W. Wang, Y. Lan, and A. Harada, "Schemes for mitigating adjacent channel interference in coexisting TDD-FDD systems," in *2013 IEEE Wireless Communications and Networking Conference (WCNC)*, April 2013, pp. 13–18.

[12] 3GPP, "Base Station (BS) radio transmission and reception (Release 12)," Tech. Rep. TS 36.104 V12.4.0, 2014.

[13] 3GPP, "User Equipment (UE) radio transmission and reception (Release 12)," Tech. Rep. TS 36.101 V12.4.0, 2014.

[14] 3GPP, "Physical layer procedures (Release 13)," Tech. Rep. TS 36.213 V13.1.1, 2016.

[15] M. Abdulla, Y. R. Shayan, and J. Baek, "Revisiting circular-based random node simulation," in *Communications and Information Technology, 2009. ISCIT 2009. 9th International Symposium on*, Sept 2009, pp. 731–732.

[16] S. Baroudi and Y. R. Shayan, "Outage probability in a circle with uniformly distributed users," in *Electrical Computer Engineering (CCECE), 2012 25th IEEE Canadian Conference on*, April 2012, pp. 1–4.

[17] 3GPP, "Small cell enhancements for E-UTRA and E-UTRAN - physical layer aspects (Release 12)," Tech. Rep. TR 36.872 v12.1.0, 2013.

[18] 3GPP, "Further advancements for E-UTRA physical layer aspects (Release 9)," Tech. Rep. TR 36.814; v9.0.0, 2010.